

RADTI: Regression Analyses of Diffusion Tensor Images

Yimei Li^a, Hongtu Zhu^{a, d}, Yasheng Chen^b, Joseph G. Ibrahim^a, Hongyu An^b, Weili Lin^{b, d},
Colin Hall^c, and Dinggang Shen^{b, d}

^aDepartment of Biostatistics, ^bDepartment of Radiology, ^cDepartment of Neurology, and
^dBiomedical Research Imaging Center, University of North Carolina at Chapel Hill, Chapel
Hill, NC 27599, USA

ABSTRACT

Diffusion tensor image (DTI) is a powerful tool for quantitatively assessing the integrity of anatomical connectivity in white matter in clinical populations. The prevalent methods for group-level analysis of DTI are statistical analyses of invariant measures (e.g., fractional anisotropy) and principal directions across groups. The invariant measures and principal directions, however, do not capture all information in full diffusion tensor, which can decrease the statistical power of DTI in detecting subtle changes of white matters. Thus, it is very desirable to develop new statistical methods for analyzing full diffusion tensors.

In this paper, we develop a set of toolbox, called RADTI, for the analysis of the full diffusion tensors as responses and establish their association with a set of covariates. The key idea is to use the recent development of log-Euclidean metric and then transform diffusion tensors in a nonlinear space into their matrix logarithms in a Euclidean space. Our regression model is a semiparametric model, which avoids any specific parametric assumptions. We develop an estimation procedure and a test procedure based on score statistics and a resampling method to simultaneously assess the statistical significance of linear hypotheses across a large region of interest. Monte Carlo simulations are used to examine the finite sample performance of the test procedure for controlling the family-wise error rate. We apply our methods to the detection of statistical significance of diagnostic and age effects on the integrity of white matter in a diffusion tensor study of human immunodeficiency virus.

Keywords: Covariate, diffusion tensor, log-Euclidean norm, regression, score statistic.

1. INTRODUCTION

Statistical analysis of diffusion tensor measures (e.g., invariant measures, eigenvalues, eigenvectors) can quantitatively assess the integrity of anatomical connectivity in white matter in the human brain in vivo (see Refs. 1, 2, 3 and 4). The simple use of invariant measures and principal directions, however, will significantly decrease the statistical power of imaging studies in detecting subtle changes of white matters. Statistical analyses of full tensors are expected to maximize our power of using diffusion tensor imaging in making valid scientific conclusions about the population under study. An appropriate statistical analysis of diffusion tensors is important for understanding normal brain development, the neural bases of neuropsychiatric disorders, and the joint effects of environmental and genetic factors on brain structure and function. In addition, any statistical method for full diffusion tensors can be directly applied to the positive-definite strain matrices in computational anatomy to understand shape variation between structural brain images; see, for example, Refs 5 and 6.

Because diffusion tensors are in a nonlinear space, it is theoretically and computationally difficult to develop a formal statistical framework, including estimation theory and hypothesis testing, for using a set of covariates to directly predict diffusion tensors as responses. One may ignore the positive definite constraint of diffusion tensors and then directly apply classical multivariate regression to studying the association between diffusion tensors and covariates. This method, however, is not adequate in practice. For instance, Ref 7 points that the simple use of the empirical average of diffusion tensors can lead to a swelling effect in imaging processing. Moreover, even when diffusion tensors are regarded as points in the nonlinear space, the existing statistical methods can only compare differences between the means of the two (or multiple) groups of diffusion tensors (see Refs. 8

Further author information: (Send correspondence to H.T. Zhu)
H.T. Zhu: E-mail: hzhu@bios.unc.edu, Telephone: 1 919 966 7272

Medical Imaging 2009: Image Processing, edited by Josien P. W. Pluim, Benoit M. Dawant,
Proc. of SPIE Vol. 7259, 72591C · © 2009 SPIE
CCC code: 1605-7422/09/\$18 · doi: 10.1117/12.812328

Proc. of SPIE Vol. 7259 72591C-1

and 4). For instance, Schwartzman 8 has developed several parametric models for diffusion tensors and derived distributions of several test statistics for testing differences in two groups of diffusion tensors.

Due to the recent development of a novel log-Euclidean metric in Ref. 9, we can transform diffusion tensors in a nonlinear space to their matrix logarithms in a Euclidean space. We develop a regression model with the log-transformed diffusion tensors as responses. Our regression model is based on a semi-parametric method, and thus it avoids specifying parametric distributions for random log-transformed diffusion tensors. We propose an inference procedure to estimate the regression coefficients in this semi-parametric model. We develop score statistics to test linear hypotheses of unknown parameters and develop a test procedure based on a resampling method to simultaneously assess the statistical significance of linear hypotheses across a large region of interest. We examine the performance of the estimation and test procedures using real imaging data. Our results show that compared with invariant measures and principal directions, full diffusion tensor is more sensitive in revealing the disruption of the integrity of white matter.

2. THEORY

Suppose we have n diffusion tensors, denoted by $\mathbf{D}_i, i = 1, \dots, n$, from a corresponding voxel in the spatially normalized and reoriented diffusion tensors images of n subjects. Subsequently, we obtain the log-transformation of \mathbf{D}_i , denoted by $\log(\mathbf{D}_i) = (Ld_{(j,k)}^i)$, and a six-dimensional vector

$$\mathbf{L}_{d,i} = [Ld_{(1,1)}^i, Ld_{(2,2)}^i, Ld_{(3,3)}^i, Ld_{(1,2)}^i, Ld_{(1,3)}^i, Ld_{(2,3)}^i]^T,$$

where $Ld_{(j,k)}^i$ denotes the (j, k) th element of the matrix logarithm of \mathbf{D}_i . For each subject, we also observe a set of clinical and behavioral variables, such as age and gender.

2.1 Model

For the log transformed diffusion tensors, we consider a linear model given by

$$\mathbf{L}_{d,i} = \beta \mathbf{x}_i + \epsilon_i \quad \text{for } i = 1, \dots, n, \quad (1)$$

where $\beta^T = [\beta_1, \dots, \beta_6]$ is a $p \times 6$ matrix representing regression coefficients and

$$\epsilon_i = [\epsilon_{(1,1)}^i, \epsilon_{(2,2)}^i, \epsilon_{(3,3)}^i, \epsilon_{(1,2)}^i, \epsilon_{(1,3)}^i, \epsilon_{(2,3)}^i]^T$$

is a 6×1 vector of measurement errors such that

$$E[\epsilon_i | \mathbf{x}_i] = \mathbf{0} \quad \text{and} \quad \text{Cov}[\epsilon_i | \mathbf{x}_i] = \Sigma, \quad (2)$$

where $E[\cdot | \mathbf{x}_i]$ and $\text{Cov}[\cdot | \mathbf{x}_i]$, respectively, denote the conditional expectation and covariance of ϵ_i given \mathbf{x}_i and Σ is a 6×6 positive definite symmetric matrix. In addition, \mathbf{x}_i is a $p \times 1$ vector containing clinical variables. For instance, if we want to compare two groups A and B, then we can set $\mathbf{x}_i = (1, \delta_A)^T$, in which 1 corresponds to intercept and δ_A is an indicator variable for group A. Specifically, in this case, model (1) can be written as

$$\mathbf{L}_{d,i} = \begin{pmatrix} \beta_{1,1} & \beta_{1,2} \\ \vdots & \vdots \\ \beta_{6,1} & \beta_{6,2} \end{pmatrix} \begin{pmatrix} 1 \\ \delta_A \end{pmatrix} + \epsilon_i, \quad (3)$$

where $\beta_{k,1}$ for $k = 1, \dots, 6$ are intercepts and $\beta_{k,2}$ for $k = 1, \dots, 6$ correspond to the differences between groups A and B in each of components of $\mathbf{L}_{d,i}$. Similarly, if we are interested in the changes of diffusion tensors across time, then we can put age into \mathbf{x}_i . Compared with general linear models, model (1) based on the conditional mean and covariance of ϵ_i avoids assuming the distributional assumption of imaging measures. It is particularly desirable for the analysis of log-transformed diffusion tensors, because the distribution of $\mathbf{L}_{d,i}$ may deviate significantly from multivariate Gaussian distribution.

Let θ be a $(6p+21) \times 1$ vector of all unknown parameters contained in β and Σ . We estimate θ by maximizing an objective function given by

$$\ell_n(\theta) = -0.5 \sum_{i=1}^n \{\log |\Sigma| + (\mathbf{L}_{d,i} - \beta \mathbf{x}_i)^T \Sigma^{-1} (\mathbf{L}_{d,i} - \beta \mathbf{x}_i)\}. \quad (4)$$

Let $\partial_\theta = \partial/\partial\theta$ denote the first partial derivative with respect to θ . Maximizing $\ell_n(\theta)$ is equivalent to solving estimating equations $\partial_\theta \ell_n(\theta) = \mathbf{0}$, which can be written as

$$\mathbf{0} = \sum_{i=1}^n (\mathbf{I}_6 \otimes \mathbf{x}_i) \Sigma^{-1} (\mathbf{L}_{d,i} - \beta \mathbf{x}_i), \quad (5)$$

$$\mathbf{0} = \Sigma - n^{-1} \sum_{i=1}^n (\mathbf{L}_{d,i} - \beta \mathbf{x}_i) (\mathbf{L}_{d,i} - \beta \mathbf{x}_i)^T, \quad (6)$$

where \otimes denotes the cross product between two matrices. Therefore, by solving $\partial_\theta \ell_n(\theta) = \mathbf{0}$, we can develop an iterative algorithm as follows:

In Step 1, we calculate the least squares estimator $\hat{\beta}_{(0)}^T = (\sum_{i=1}^n \mathbf{x}_i \mathbf{x}_i^T)^{-1} \sum_{i=1}^n \mathbf{x}_i \mathbf{L}_{d,i}^T$, and then we substitute $\hat{\beta}_{(0)}$ into (6) to get $\hat{\Sigma}_{(0)} = n^{-1} \sum_{i=1}^n (\mathbf{L}_{d,i} - \hat{\beta}_{(0)} \mathbf{x}_i)^{\otimes 2}$, where $\mathbf{a}^{\otimes 2} = \mathbf{a} \mathbf{a}^T$ for a vector \mathbf{a} . Set $t = 1$.

In Step 2, we solve $\hat{\beta}_{(t)}$ from (5) with $\Sigma = \hat{\Sigma}_{(t-1)}$, and then update $\hat{\Sigma}_{(t)} = n^{-1} \sum_{i=1}^n (\mathbf{L}_{d,i} - \hat{\beta}_{(t)} \mathbf{x}_i)^{\otimes 2}$ according to (6).

In Step 3, we increase $t = t + 1$ and go back to Step 2. The algorithm stops until the absolute difference between consecutive $\hat{\theta}^{(t)}$ s is smaller than a predefined small number, say 10^{-4} .

2.2 Hypotheses and Test Statistics

In real applications, it is common to test linear hypotheses of β in order to answer various scientific questions involving a comparison of diffusion tensors across two (or more) diagnostic groups or the changes of diffusion tensors across time. See, for example, in Refs. 6, 8 and 4. We can formulate these questions as testing linear hypotheses of θ as follows:

$$H_0 : R\beta^V = \mathbf{b}_0 \quad \text{vs.} \quad H_1 : R\beta^V \neq \mathbf{b}_0, \quad (7)$$

where $\beta^V = [\beta_1^T, \dots, \beta_6^T]^T$ is a $6p \times 1$ vector, R is an $r \times 6p$ matrix of full row rank and \mathbf{b}_0 is an $r \times 1$ specified vector. For instance, if we want to compare diffusion tensors between groups A and B in model (3), then we have

$$R = \begin{pmatrix} 0 & 1 & 0 & 0 & 0 & 0 & 0 & 0 & 0 & 0 & 0 & 0 & 0 \\ 0 & 0 & 0 & 1 & 0 & 0 & 0 & 0 & 0 & 0 & 0 & 0 & 0 \\ 0 & 0 & 0 & 0 & 0 & 1 & 0 & 0 & 0 & 0 & 0 & 0 & 0 \\ 0 & 0 & 0 & 0 & 0 & 0 & 0 & 1 & 0 & 0 & 0 & 0 & 0 \\ 0 & 0 & 0 & 0 & 0 & 0 & 0 & 0 & 0 & 1 & 0 & 0 & 0 \\ 0 & 0 & 0 & 0 & 0 & 0 & 0 & 0 & 0 & 0 & 0 & 1 & 0 \end{pmatrix} \quad \text{and} \quad \mathbf{b}_0 = \mathbf{0}_6, \quad (8)$$

where $\mathbf{0}_6$ is a 6×1 vector of zeros.

We test the null hypothesis $H_0 : R\beta^V = \mathbf{b}_0$ using a score test statistic S_n defined by

$$S_n = \partial_\mu L_n^T \hat{\mathbf{I}}_{\mu\mu}^{-1} \partial_\mu L_n, \quad (9)$$

where $\mu = R\beta^V$, $\partial_\mu L_n = n^{-1/2} \sum_{i=1}^n U_{i,\mu}(\tilde{\theta})$ and $\hat{\mathbf{I}}_{\mu\mu} = n^{-1} \sum_{i=1}^n [U_{i,\mu}(\tilde{\theta}) - \bar{U}_\mu(\tilde{\theta})][U_{i,\mu}(\tilde{\theta}) - \bar{U}_\mu(\tilde{\theta})]^T$, in which $\bar{U}_\mu(\tilde{\theta}) = \sum_{i=1}^n U_{i,\mu}(\tilde{\theta})/n$ and $\tilde{\theta}$ maximizes $\ell_n(\theta)$ under the linear constraints $R\beta^V = \mathbf{b}_0$. Solving $\tilde{\theta}$ can be done using the Lagrange multiplier method. Exact formula for $\partial_\mu L_n$ can be found in Ref. 10. Particularly, $\hat{\mathbf{I}}_{\mu\mu}$ is an estimator of the covariance matrix of $\partial_\mu L_n$ and $\hat{\mathbf{I}}_{\mu\mu}^{-1/2} \partial_\mu L_n$ is approximately a Gaussian random vector having a zero mean vector and an identity covariance matrix under $H_{0,\mu}$. Thus, the statistic S_n is approximately distributed as $\chi^2(r)$, a chi-square distribution with r degrees of freedom (see Ref. 11).

2.3 Test Procedure

In neuroimaging studies, we are often interested in testing the null hypotheses in all voxels d of the region \mathcal{D} under study. In the following, we will introduce voxel d into all mathematical notation, if necessary. To control the family-wise error rate, we consider the maxima of the score test statistics, defined by $S_{\mu, \mathcal{D}} = \max_{d \in \mathcal{D}} S_n(d)$.

To use $S_{\mu, \mathcal{D}}$ as test statistics, we need to know its distributions under the null hypothesis across all voxels of the relevant region. We present a test procedure that is based on the resampling method to approximate the distribution of $S_{\mu, \mathcal{D}}$ (see Refs. 10, 12 and 13). This procedure is essentially a wild bootstrap method for hypothesis test. The test procedure is implemented as follows:

Step 1: At each voxel d , calculate the score test statistic $S_n(d)$ given in (9), and then compute $S_{\mu, \mathcal{D}} = \max_{d \in \mathcal{D}} S_n(d)$;

Step 2: Generate a random sample $\{\eta_i^{(s)} : i = 1, \dots, n\}$ from the distribution F , which is defined by $\eta_i^{(s)} = \pm 1$ with equal probability.

Step 3: At each voxel d of \mathcal{D} , calculate

$$S_n(d)^{(s)} = \partial_{\mu} L_n(d)^{(s)T} [\tilde{\mathbf{I}}_{\mu\mu}(d)]^{-1} \partial_{\mu} L_n(d)^{(s)}$$

and then compute $S_{\mu, \mathcal{D}}^{(s)} = \max_{d \in \mathcal{D}} S_n(d)^{(s)}$, where

$$\partial_{\mu} L_n(d)^{(s)} = n^{-1/2} \sum_{i=1}^n U_{i, \mu}(\tilde{\theta}, d) \eta_i^{(s)} \text{ and } \tilde{\mathbf{I}}_{\mu\mu}(d) = n^{-1} \sum_{i=1}^n [U_{i, \mu}(\tilde{\theta}, d)]^{\otimes 2}.$$

Step 4: Repeat Steps 2-3 S times to obtain $\{S_{\mu, \mathcal{D}}^{(s)} : s = 1, \dots, S\}$. Finally, the p value of $S_{\mu, \mathcal{D}}$ is approximated by

$$p_{\mu, \mathcal{D}} = S^{-1} \sum_{s=1}^S 1(S_{\mu, \mathcal{D}}^{(s)} \geq S_{\mu, \mathcal{D}}).$$

If $p_{\mu, \mathcal{D}}$ is smaller than a pre-specified value α , say 0.05, then we reject that the null hypothesis $H_0 : R\beta^V = \mathbf{b}_0$ holds across all voxels of the region \mathcal{D} .

Step 5: Calculate the p -value of $S_n(d)$ at each voxel d of the region according to

$$p(d) \approx S^{-1} \sum_{s=1}^S 1(S_n(d)^{(s)} \geq S_n(d)).$$

Step 6: Calculate the corrected p -value of $S_n(d)$ at each voxel d of the region using

$$p_D(d) \approx S^{-1} \sum_{s=1}^S 1(S_{\mu, \mathcal{D}}^{(s)} \geq S_n(d)).$$

We note several advantages of using the resampling method in the above test procedure. Computationally, the above procedure only requires the computation of $\hat{U}_{i, \mu}(\tilde{\theta}, d)$ once and the repeated calculation of $S_n(d)^{(s)}$. Thus, because the permutation method involves refitting the model for each simulated data, the proposed test procedure is computationally much more efficient than the permutation method. Moreover, permutation methods require "complete exchangeability" condition, which is a very strong assumption particularly in the presence of clinical variables as pointed out by Refs. 10 and 14.

3. HIV DTI DATA

We assess the integrity of white matter in human immunodeficiency virus (HIV). White matter is one of the three main solid components of the central nervous system (CNS) and is composed of bundles of myelinated nerve cell processes (or axons), which connect various gray matter areas (the locations of nerve cell bodies) of the brain to each other, and carry nerve impulses between neurons. The white matter is important for passing messages between different areas of gray matter within the CNS. After initial HIV infection, the virus is detectable in the CNS before antibodies are detectable in the blood and HIV could be cultured from brain tissue as early as fifteen days (see Refs. 15). Since DTI can detect the subtle disruption of white matter structural integrity by assessing the degree to which fiber tracts within the white matter have lost their directional organization (see Refs. 1, 2, 3, 16 and 17), DTI may be an important tool for detecting the early CNS HIV involvement.

We applied our statistical methods to assess statistically significant effects of diagnosis and age on the integrity of white matter in a cross-sectional study of human immunodeficiency virus (HIV). This dataset has 29 HIV+ subjects (21 males and 8 females; age mean: 40.0, SD: 5.6 years) and 18 healthy (9 males and 9 females; age mean: 41.2, SD: 7.4 years) controls. Diffusion-weighted images and T1 weighted images were acquired for each subject. Diffusion tensor acquisition scheme includes 18 repeated measures of six non-collinear directions, (1,0,1), (-1,0,1), (0,1,1), (0,1,-1), (1,1,0), and (-1,1,0) at a b-value of 1000 s/mm² and a b=0 reference scan. Forty-six contiguous slices with a slice thickness of 2 mm covered a field of view (FOV) of 256 mm² with an isotropic voxel size of 2 × 2 × 2 mm³. High resolution T1 weighted (T1W) images were acquired using a 3D MP-RAGE sequence. A weighted least square estimation method as investigated in Refs. 2 and 18 was used to construct the diffusion tensors.

The normalization of DTIs of different HIV individuals is completed by a recently developed DTI registration algorithm (See Ref. 19) which uses regional tensor distribution information and local boundaries, both extracted directly from the tensors, to hierarchically guide the alignment of DTIs. This is in contrast with conventional methods which typically compute regional and edge information based on tensor scalar maps, which might not necessarily reflect the actual tensor information. In our method, for each voxel, the statistical measures such as mean and variance are computed in various neighborhood sizes to extract multiscale tensor information. Edge boundaries are obtained by an extended Canny edge detector which works directly on the tensors. Then distinctive features are selected hierarchically as landmark points to guide the registration. The performance of this method has been compared with others (See Refs. 20 and 21), indicating better performance in estimating simulated brain deformations and atrophies (See Refs. 19 and 22).

Fractional anisotropy (FA) calculated from DTIs is widely used as measurement to assess directional organization of the brain which is greatly influenced by the magnitude and orientation of white matter tracts. However, FA measures do not capture all information in full diffusion tensor and thus can decrease the statistical power in detecting subtle changes of white matters. To demonstrate the advantage of the analysis of the the full diffusion tensors as response versus the analysis of the FA as responses, we implemented two analyses in which applied the semiparametric model described above at each voxel for full diffusion tensors and general linear model for FA measures respectively. In the first analysis, full diffusion tensors were treated as response and we considered model (1), in which $\mathbf{x}_i = (1, \delta_{HIV}, \text{age}, \text{gender})^T$, at each voxel, where δ_{HIV} equals 1 for HIV+ and 0 for Healthy control and gender equals 1 for female and 0 for male. Here, R is a 6×24 matrix and $b_0 = (0, 0, 0, 0, 0, 0)^T$ for the hypotheses on either diagnosis or age. In the second analysis, FA measurements were treated as response and $\mathbf{x}_i = (1, \delta_{HIV}, \text{age}, \text{gender})^T$ was still considered as covariates in the general linear model. Standard analysis was performed to detect the statistical significance of diagnosis or age.

The uncorrected p -values based on the score test statistics for diagnostic effects were color-coded at each voxel in white matter area of the reference brain for two analyses respectively (Fig. 1(a) and (b)). To correct for multiple comparison, we applied our test procedure to calculated the adjusted p -value $p_D(d)$ map (Fig. 1(c) and (d)). Color-coded maps of p -values using either the uncorrected $p(d)$ alone or the corrected $p_D(d)$ indicated the different performances of these two analyses. The analysis in which full diffusion tensor used as response provides more information and has stronger statistical power for detecting the disruption of white matter integrity in HIV individuals compared with that based on FA (Fig. 1(b) and (d)). Similarly, color-coded maps of p -values using either the uncorrected $p(d)$ alone or the corrected $p_D(d)$ for age effect were calculated for both analyses (Fig. 2). The advantage of using full diffusion tensor as response to detect the subtle changes of white matters. More

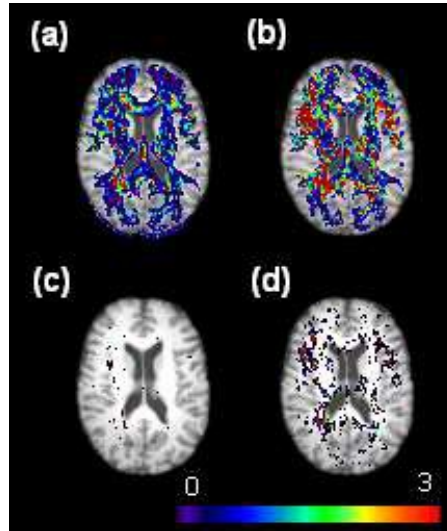


Figure 1. Diagnostic effect results from HIV+ data set. Panels (a) and (c) present color-coded maps of raw (a) and adjusted (b) $-\log_{10}(p)$ values in a selected ROI of the template when modeling FA as response variable. Panels (b) and (d) present color-coded maps of raw (b) and adjusted (d) $-\log_{10}(p)$ values in a selected ROI of the template when modeling full diffusion tensor as response variable. The color scale reflects the magnitude of values of $-\log_{10}(P)$ with black to blue representing smaller values (0-1) and red to white representing larger values (1.88-3).

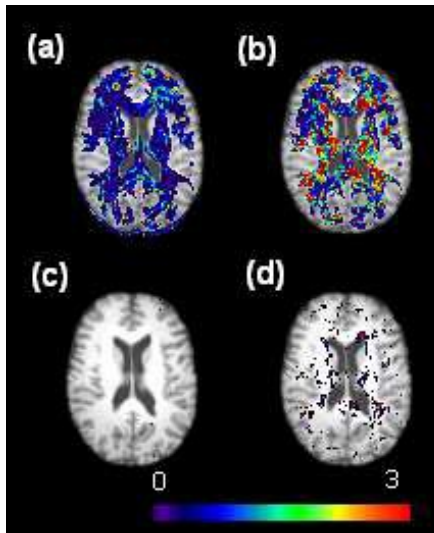


Figure 2. Age effect results from HIV+ data set. Panels (a) and (c) present color-coded maps of raw (a) and adjusted (b) $-\log_{10}(p)$ values in a selected ROI of the template when modeling FA as response variable. Panels (b) and (d) present color-coded maps of raw (b) and adjusted (d) $-\log_{10}(p)$ values in a selected ROI of the template when modeling full diffusion tensor as response variable. The color scale reflects the magnitude of values of $-\log_{10}(P)$ with black to blue representing smaller values (0-1) and red to white representing larger values (1.88-3).

regions are identified as significantly regions for the age effect when full diffusion tensor were treated as response (Fig. 2(b) and (d)). We also chose a single voxel and used an ellipsoid representation to display diffusion tensors for all subjects (Fig. 3). We observed the difference of age trend between two groups.

DISCUSSION

We have developed a general statistical framework for the regression model of log-transformed diffusion

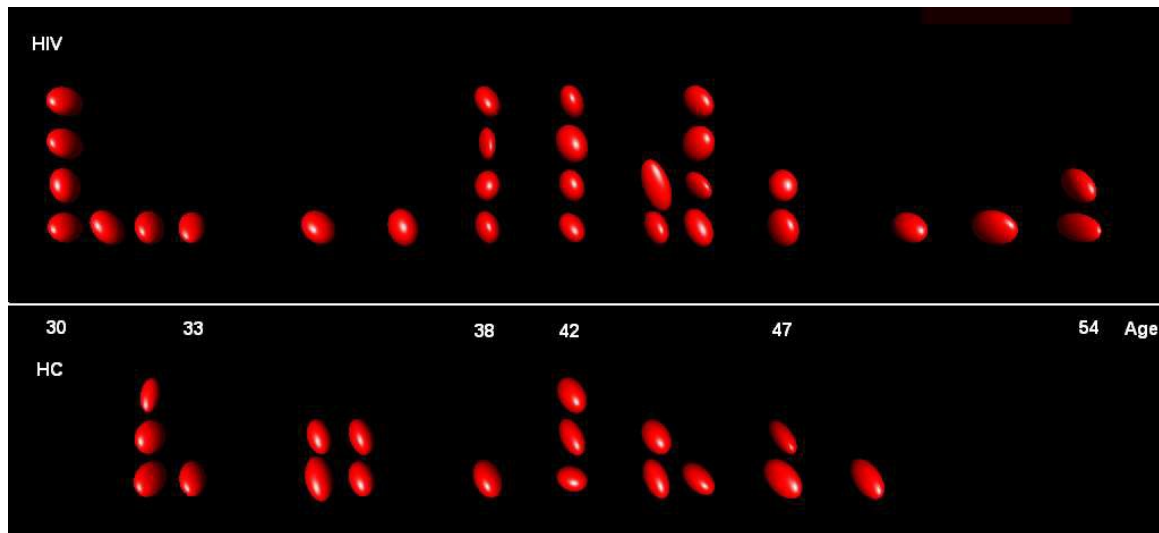


Figure 3. Ellipsoid representation of diffusion tensors from a single voxel to illustrate significant effects of age.

tensors and their association with a set of covariates. The regression model proposed here avoids any parametric assumptions regarding log-transformed diffusion tensors. We have examined our estimation and test procedures for carrying out statistical inference using simulated data and neuroimaging data. We expect a great clinical application of this novel statistical technique. A toolbox for implementing RADTI is available upon request and a complete version will be released on <http://www.nitrc.org/> soon.

ACKNOWLEDGMENTS

This work was supported in part by NSF grants SES-06-43663 and BCS-08-26844 and NIH grants UL1-RR025747-01 and R21AG033387 to Dr. Zhu, NIH grants GM 70335 and CA 74015 to Dr. Ibrahim, NIH grant R01NS055754 to Dr. Lin, and NIH grant 1R01EB006733 to Dr. Shen.

REFERENCES

- [1] Basser, P. J., Mattiello, J., and LeBihan, D., "Mr diffusion tensor spectroscopy and imaging," *Biophysical Journal* **66**, 259–267 (1994).
- [2] Basser, P. J., Mattiello, J., and LeBihan, D., "Estimation of the effective self- diffusion tensor from the nmr spin echo," *Journal of Magnetic Resonance Ser. B* **103**, 247–254 (1994).
- [3] Lim, K. O. and Helpert, J. A., "Neuropsychiatric applications of dti - a review," *NMR in Biomedicine* **15**, 587–593 (2002).
- [4] Whitcher, B., Wisco, J., Hadjikhani, N., and Tuch, D. S., "Statistical group comparison of diffusion tensors via multivariate hypothesis testing," *Magnetic Resonance in Medicine* **57**, 1065–1074 (2007).
- [5] Grenander, U. and Miller, M. I., "Computational anatomy: an emerging discipline," *Quarterly of Applied Mathematics* **56**, 617–694 (1998).
- [6] Lepore, N., Brun, C. A., Chou, Y., Chiang, M., Dutton, R. A., Hayashi, K. M., Luders, E., Lopez, O. L., Aizenstein, H. J., Toga, A. W., Becker, J. T., and Thompson, P. M., "Generalized tensor-based morphometry of hiv/aids using multivariate statistics on deformation tensors," *IEEE Transactions in Medical Imaging* **27**, 129–141 (2008).
- [7] Chéfd'hotel, C., Tschumperlé, D., Deriche, R., and Faugeras, O., "Regularizing flows for constrained matrix-valued images," *Journal of Mathematical Imaging and Vision* **20**, 147–162 (2004).
- [8] Schwartzman, A., *Random Ellipsoids and False Discovery Rates: Statistics for Diffusion Tensor Imaging Data*, PhD thesis, Stanford University, California (July 2006).

- [9] Arsigny, V., Fillard, P., Pennec, X., and Ayache, N., “Log-euclidean metrics for fast and simple calculus on diffusion tensors,” *Magnetic Resonance in Medicine* **56**, 411–421 (2006).
- [10] Lin, D. Y., “An efficient monte carlo approach to assessing statistical significance in genomic studies,” *Bioinformatics* **6**, 781–787 (2005).
- [11] Lehmann, E. L. and Romano, J. P., [*Testing Statistical Hypotheses*], Springer-Verlag, New York (2006).
- [12] Zhu, H. T., Li, Y. M., Tang, N. S., Bansal, R., Hao, X. J., Weissman, M. M., and Peterson, B. G., “Statistical modelling of brain morphological measures within family pedigrees,” *Statistica Sinica* **18**, 1554–1569 (2008).
- [13] Kosorok, M. R., “Bootstraps of sums of independent but not identically distributed stochastic processes,” *J. Multivariate Anal.* **84**, 299–318 (2003).
- [14] Dudoit, S., Shaffer, J. P., and Boldrick, J. C., “Multiple hypothesis testing in microarray experiments,” *Statist. Sci.* **18**, 71–103 (2003).
- [15] Rausch, D. M. and Davis, M. R., “Hiv in the cns: pathogenic relationships to systemic hiv disease and other cns diseases,” *J. Neurovirol.* **7**, 85–96 (2001).
- [16] Vernooij, M. W., de Groot, M., van der Lugt, A., Ikram, M. A., Krestin, G. P., Hofman, A., Niessen, W. J., and Breteler, M. M. B., “White matter atrophy and lesion formation explain the loss of structural integrity of white matter in aging,” *NeuroImage* **43**, 407–477 (2008).
- [17] Focke, N. K., Yogarajah, M., Bonelli, S. B., Bartlett, P. A., Symms, M. R., and Duncan, J. S., “Voxel-based diffusion tensor imaging in patients with mesial temporal lobe epilepsy and hippocampal sclerosis,” *NeuroImage* **40**, 728–737 (2008).
- [18] Zhu, H. T., Zhang, H. P., Ibrahim, J. G., and Peterson, B. G., “Statistical analysis of diffusion tensors in diffusion-weighted magnetic resonance image data (with discussion),” *Journal of the American Statistical Association* **102**, 1085–1102 (2007).
- [19] Yap, P.-T., Zhu, H., Lin, W., and Shen, D., “Hierarchical diffusion tensor image registration based on tensor regional distributions,” in *ISMRM* (2009).
- [20] Yang, J., Shen, D., Misra, C., Wu, X., Resnick, S., Davatzikos, C., and Verma, R., “Spatial normalization of diffusion tensor images based on anisotropic segmentation,” in *SPIE Medical Imaging, San Diego* (2008).
- [21] Zhang, H., Yushkevich, P. A., Alexander, D. C., and Gee, J. C., “Deformable registration of diffusion tensor mr images with explicit orientation optimization,” *Medical Image Analysis* **10**, 764–785 (2006).
- [22] Yap, P.-T., Zhu, H., Lin, W., and Shen, D., “Timer: Tensor image morphing for elastic registration,” *Neuroimage* (2009).